JOURNAL OF MATERIALS SCIENCE 27 (1992) 358–364

Structural evolution of alumina–γ-aluminium oxynitride composites during high-temperature compression creep

D. GOEURIOT-LAUNAY, P. GOEURIOT, F. THEVENOT
Laboratoire des Céramiques Spéciales, ENSMSE, 158 cours Fauriel, 42023 Saint-Etienne Cédex 2, France

C. CARRY
Laboratoire de Céramiques, EPFL, MX.D Ecublens, CH1015, Lausanne, Switzerland

TEM studies of Al_2O_3–γ-AlON composites show the presence of precipitates in the γ-AlON phase, due to a partial decomposition of this metastable phase formed during heat treatment. Thermal treatment (1650 °C) has no effect on the microstructure, while compressive creep deformation (1650 °C, 10–30 MPa) leads to a decrease of the γ-AlON content. This phase decomposes, probably into alumina or alumina-poor AlON. The precipitation process can be activated by the presence of dislocations, and is associated with a slight increase in strain rate during creep.

1. Introduction

Recent studies [1, 2] showed that the addition of γ-aluminium oxynitride (γ-AlON) in an alumina matrix has an interesting effect on some of its properties. The presence of γ-AlON in the alumina matrix improves its wear resistance [3]. At room temperature such composites have the same mechanical properties as alumina, but the γ-spinel phase limits grain boundary sliding in the temperature range 1100–1500 °C; this mechanism leads to macroplasticity in fine-grained alumina material tested under creep conditions, so that flexural strengths of the composites are maintained above 1000 °C [2, 4]. The toughness values are also maintained and even increased for high γ-AlON contents (30–40 vol %).

Recently it has been shown that fine-grained ceramics can exhibit superplastic behaviour at high temperature under rather low stresses, and elongations to rupture higher than 100% have been reported [5]. As for metallic materials, the presence of a second phase limits grain growth phenomena in ceramics and generally improves the superplastic behaviour of such materials. In this way plastic deformation up to 500% has been obtained in fine-grained alumina–zirconia composites [6]. During superplastic deformation of single-phase ceramics or composite materials [6, 7], various structural evolutions can be observed: enhanced grain growth [8], cavity nucleation and growth, some crystallographic texture and in some cases grain elongation or even recrystallization as observed in spinels [9].

This work has been undertaken to see if such superplastic behaviour could be observed in alumina–γ-aluminium oxynitride composites. The structural evolutions have been studied during thermomechanical treatment to separate the strain/stress effects on microstructure from the influence of temperature alone. Composite materials with different nominal volume fractions of AlON were tested between 20 and 35 MPa. Macroscopic flow behaviour under creep conditions was studied by the strain rate (ε) evolution for constant stress tests and by measuring the stress exponent of the relationship $\dot{\varepsilon} = f(\sigma^n)$ with stress jump experiments. Structural evolution during thermomechanical treatment is characterized in terms of cavitation (density loss), grain size, crystallographic texture and γ-AlON volume fraction which can vary because of initial Al_2O_3 enrichment of this phase.

2. Experimental procedure

The composite materials were obtained by uniaxial hot-pressing of Al_2O_3–AlN mixtures. With regard to the phase diagram established by McCauley and Corbin [10] the initial AlN contents in the powder mixtures were chosen to prepare composites with 10, 20 and 30 vol % of AlON. Hot-pressed disks were of 30 mm in diameter and 12 mm height. The real AlON volume fractions were deduced from the measured densities of the hot-pressed disks, assuming that they are fully dense (with $\rho_{Al_2O_3} = 3.987\ g\,cm^{-3}$ and $\rho_{AlON} = 3.65\ g\,cm^{-3}$).

Microstructures were observed on polished and thermally etched surfaces parallel to the pressing direction and to the uniaxial creep stress after deformation. Thermal etching conditions (1450 °C, 2 min in flowing H_2) made the AlON phase appear with a light grey colour on scanning electron micrographs.

X-ray diffraction (XRD) spectra were obtained on polished surfaces parallel to the hot-pressing stress

0022-2461/92 $03.00 + .12

direction and perpendicular to that of uniaxial creep stress. Two different ratios calculated from X-rays peak heights are used: τ to follow the evolution of the γ-AlON content, and R to follow the crystallographic texture evolution of the Al_2O_3 phase:

$$\tau = \frac{I_{400}^{\mathrm{AlON}} + I_{220}^{\mathrm{AlON}}}{I_{113}^{\mathrm{Al_2O_3}} + I_{104}^{\mathrm{Al_2O_3}}} \times 100$$

$$R = \frac{(I_{1010}/\sum I_{hkil})\mathrm{Al_2O_3}(\text{hot pressed})}{(I_{1010}/\sum I_{hkil})\mathrm{Al_2O_3}(\text{powder})}$$

R is a normalized peak intensity ratio [11] for the 1 0 1 0 crystallographic plane of the α-Al_2O_3 structure marking a small angle with its basal plane.

Transmission electron microscopy (TEM) observations were made on ion-milled thin foils sputtered with carbon and using a 200 kV electron microscope (Hitachi H800).

Creep experiments were performed either under constant stress or with some stress jumps to estimate the stress exponent n. A reference sample (labelled T) was systematically positioned next to the creeping sample so as to be subjected to the same heat treatment but in a stress-free condition. Other details of creep conditions have been described elsewhere [7, 8]. Samples were parallelepipeds with dimensions 24 mm × 8 mm × 8 mm.

3. Materials and creep behaviour

Table I presents the preparation conditions and characteristics of the hot-pressed materials to be thermomechanically treated.

Fig. 1 shows the microstructures of the three materials. A remarkable fact can be pointed out: while Al_2O_3 and AlN powders have been mixed in proportions to obtain materials with 10, 20 and 30% volume fraction of AlON for respectively A, B, and C materials, the density measurements, the microstructure observations and the τ X-ray ratios clearly indicate a much higher fraction of AlON for B and C materials. Previous work [1] showed that the AlON content increases with sintering temperature. These observations contradict the verticality of the Al_2O_3-rich limit composition of the γ-oxynitride in the phase diagram

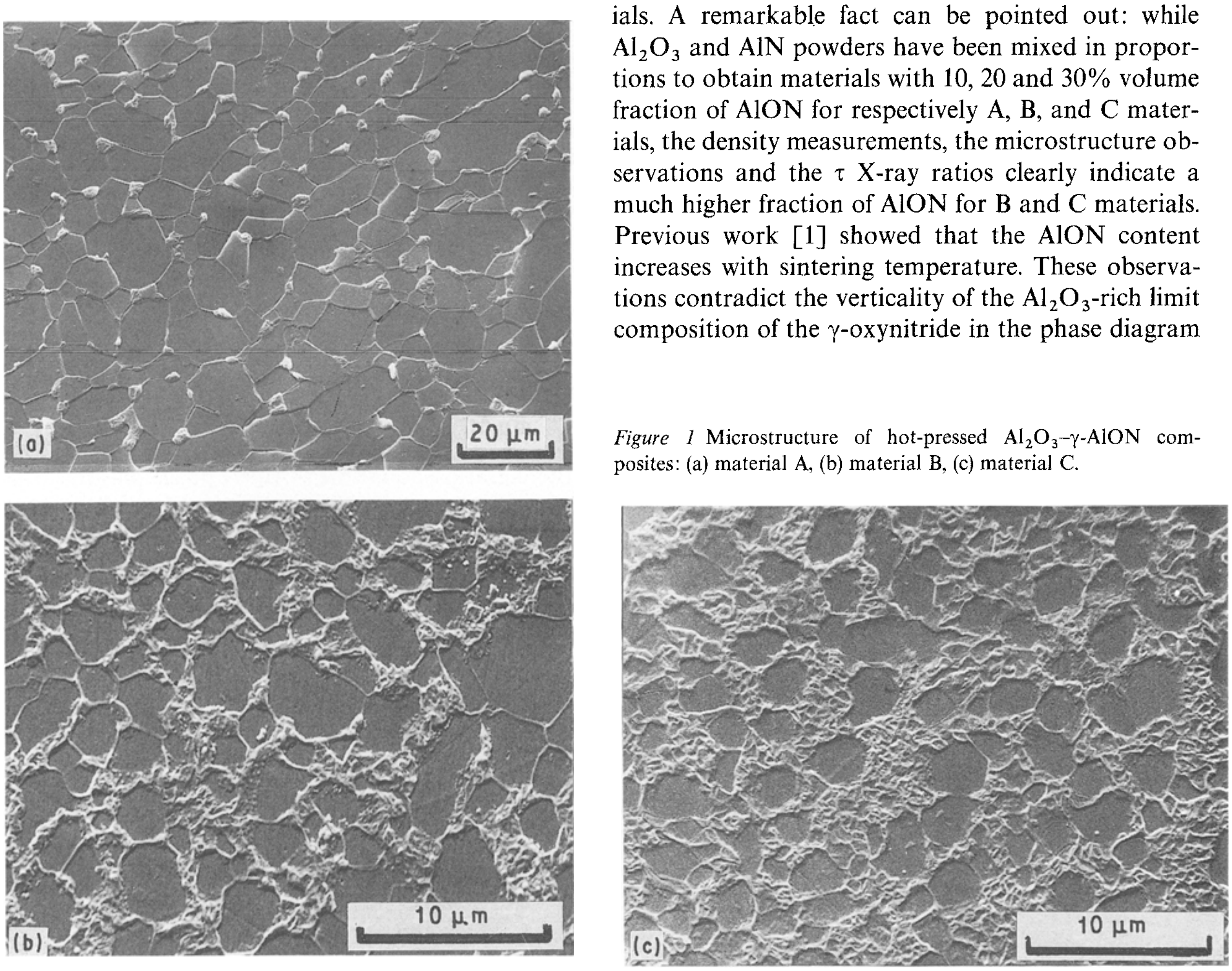

Figure 1 Microstructure of hot-pressed Al_2O_3–γ-AlON composites: (a) material A, (b) material B, (c) material C.

TABLE I Preparation and characterization of Al_2O_3–γ-AlON composites

Material	Powders (wt %)		Hot-pressing conditions			Density	τ	AlON (vol %)	Al_2O_3 grain size (µm)	R_{1010}
	Al_2O_3	AlN[‡]	T(°C)	P(MPa)	t(min)	(gcm^{-3})				
A	98.45*	1.55	1800	15	30	3.956	3.5	10	10	0.68
B	96.88*	3.12	1800	15	30	3.885	11.4	33	5	0.68
C	95.52[†]	4.48	1820	15	30	3.810	23.1	55	3	0.85

* Al_2O_3 A6Z, Criceram (France).
[†] Al_2O_3 GE6, Baikowski (France).
[‡] AlN S, Starck (Germany).

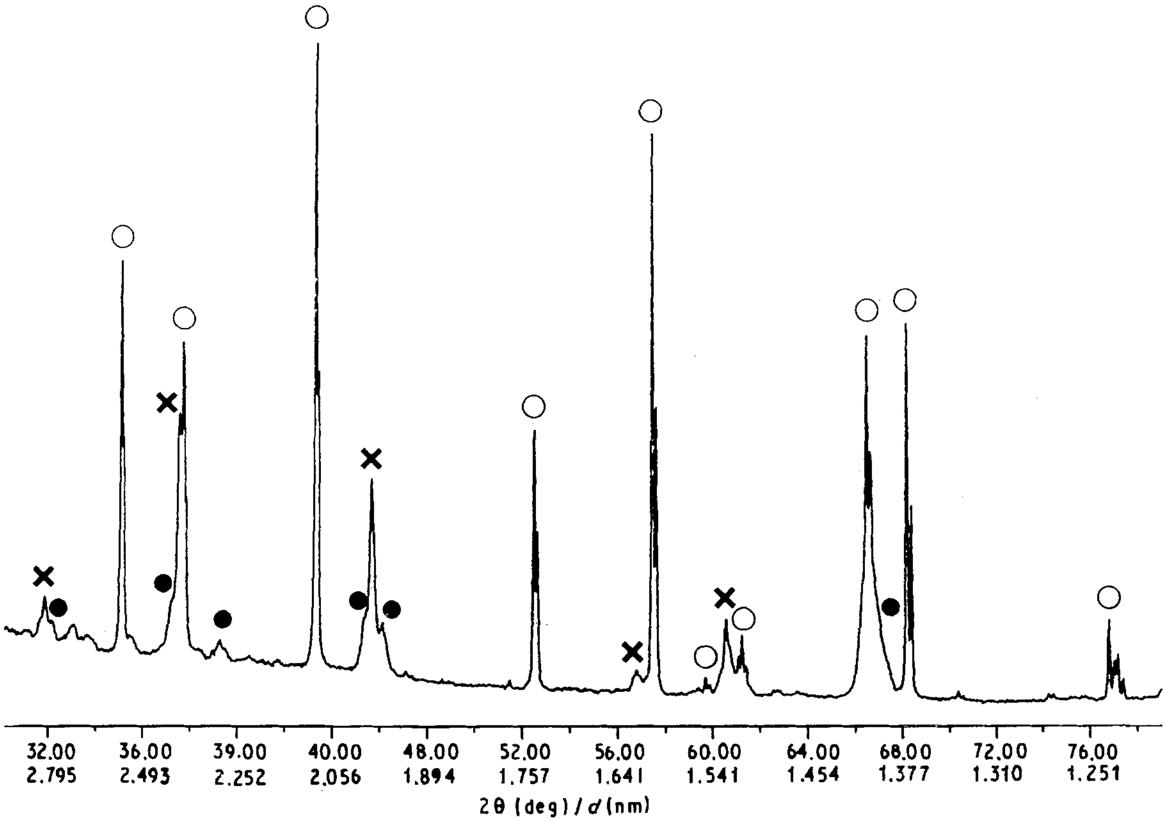

Figure 2 X-ray spectrum of material illustrating the high volume fraction of AlON and the presence of δ-oxynitride phase: (○) Al_2O_3, (×) γ-AlON, (●) δ-AlON.

proposed by McCauley and Corbin [10]. They are in good agreement with the results of Bassoul *et al.* [12] who showed the possibilities of synthetizing a spinel oxynitride containing up to 80 or 85 mol% Al_2O_3. However, according to Bassoul *et al.* this Al_2O_3-rich spinel is metastable and thermal treatments can decompose it into alumina and an AlON spinel phase with a low Al_2O_3 content. Taking account of the sintering temperature of the samples (1800 °C), this means that at the creep temperature (1650 °C) the γ-AlON phase which must be rich in Al_2O_3 should be metastable and could decompose. Material C (Table I) also presents some δ (tetragonal) oxynitride (Fig. 2). In the as-hot-pressed materials two kinds of AlON grain are observed: polygonal grains at alumina triple junctions, and more elongated grains along some Al_2O_3 grain boundaries. The alumina grain size decreases as the γ-AlON content increases; this clearly illustrates the limiting effect of second phase on the Al_2O_3 grain growth during sintering. The *R* values lower than unity indicate a slight basal texture perpendicular to the pressing direction.

Creep curves ($\dot{\varepsilon}$ versus ε) of these composites are represented in Fig. 3. Contrary to fine-grained single-phase alumina [7, 8] for which strain rates decrease continuously due to grain growth, the strain rates can be considered as constant or even lightly increasing from the beginning of the test. As for other ceramic composites or biphased superplastic metals, a kind of steady state (constant strain rate) is observed with a low softening effect (increasing strain rate). The low stress exponents ($1.5 < n < 2$), the strain rate range ($10^{-5} < \dot{\varepsilon} < 10^{-4}$) and the levels of deformation without macroscopic damage are characteristic of superplastic behaviour. The alumina grain size varies from one material to the other and nothing is available in the literature about the γ-AlON phase plasticity, so it is rather difficult to discuss the effect of AlON volume fraction on the deformability of such composites. The conclusion is that about 30% AlON volume fraction could be an optimum to easily reach high deformation levels.

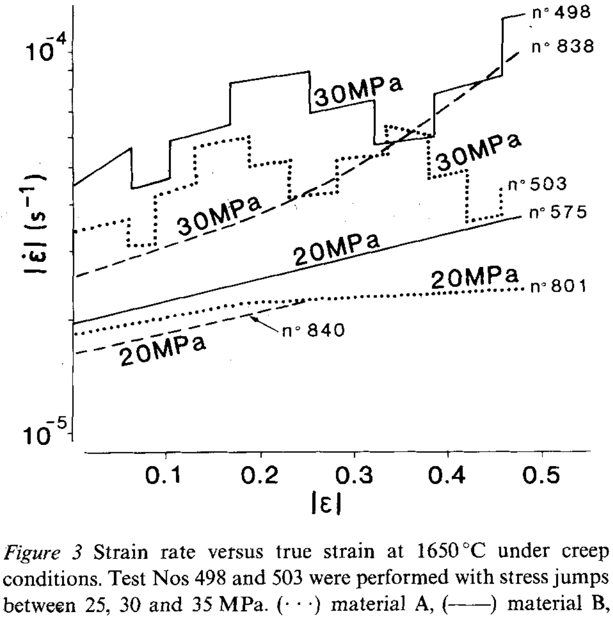

Figure 3 Strain rate versus true strain at 1650 °C under creep conditions. Test Nos 498 and 503 were performed with stress jumps between 25, 30 and 35 MPa. (· · ·) material A, (——) material B, (– –) material C.

TABLE II Characterization of composite samples after thermomechanical treatment at 1650 °C*

Material	Test No.	Stress (MPa)	Final true strain	Time at 1650 °C (min)	Density variation, 100 $(\rho_D - \rho_T)/\rho_T$	τ_T	τ_D	R_D
A	801	20	−0.486	366	−5.43	–	0.52	2.91
	503	30	−0.486	172	−6.87	1.1	1.2	2.56
B	575	20	−0.475	300	+ 0.31	10.5	6.8	1.17
	498	30	−0.485	122	−1.11	10.4	8.4	0.99
C	840	20	−0.25	225	+3.5	21.7	22.2	0.827
	838	30	−0.47	185	+4.01	19.9	18.1	0.915

* D and T subscripts refer to deformed samples and stress-free annealed samples, respectively.

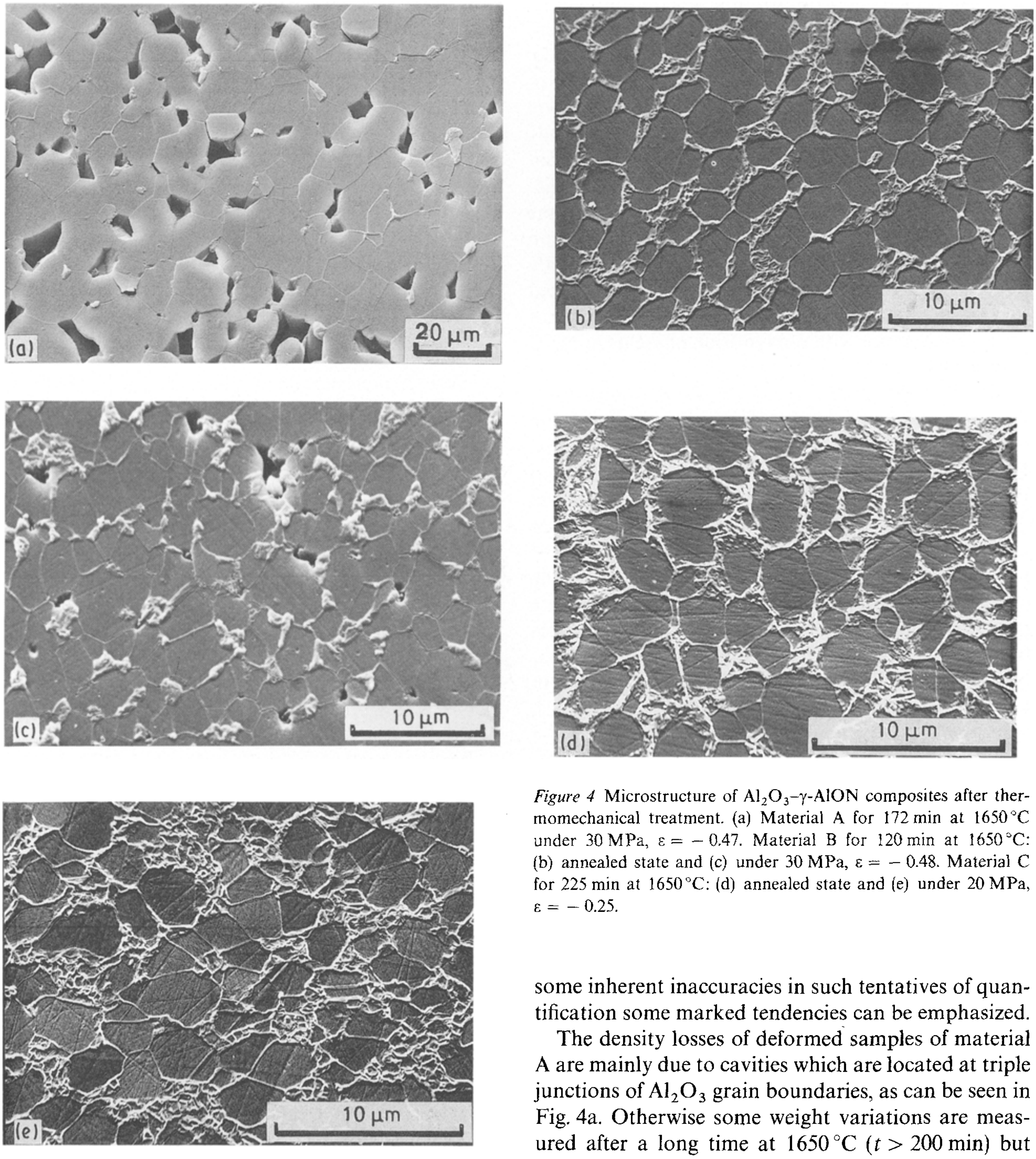

Figure 4 Microstructure of Al_2O_3–γ-AlON composites after thermomechanical treatment. (a) Material A for 172 min at 1650 °C under 30 MPa, ε = − 0.47. Material B for 120 min at 1650 °C: (b) annealed state and (c) under 30 MPa, ε = − 0.48. Material C for 225 min at 1650 °C: (d) annealed state and (e) under 20 MPa, ε = − 0.25.

4. Structural evolution, interpretation and discussion

Table II presents the variations of density and X-rays parameters τ and *R* for samples of the three composites after thermomechanical treatment. Despite some inherent inaccuracies in such tentatives of quantification some marked tendencies can be emphasized.

The density losses of deformed samples of material A are mainly due to cavities which are located at triple junctions of Al_2O_3 grain boundaries, as can be seen in Fig. 4a. Otherwise some weight variations are measured after a long time at 1650 °C ($t > 200$ min) but annealed and deformed samples are identically affected. Such cavities probably result from the non-accommodation of grain boundary sliding: such a mechanism is more important in larger-grain material such as A compared to B and C composites. In addition to this cavitation the significant development of a basal texture perpendicular to the uniaxial creep stress can be noted. Such a texture could result from the activation of basal slide in this larger-grain material: the creep stresses imposed for these tests were higher than the stress necessary to activate basal dislocation slides in alumina at 1650 °C [11]. In material with a rather low AlON fraction the overall deformation would result from grain boundary sliding more or less well accommodated by transgranular dislocation plasticity and by cavitation.

For materials of higher AlON content (B and C) no significant basal crystallographic texture and cavitation are observed, but X-ray analysis and micrographs (Table II and Fig. 4) show a significant AlON content decrease after thermomechanical treatment; this phenomenon is much more important in deformed samples of B material than in C. The microstructures of the stress-free annealed samples are similar to those of the initial composites (Fig. 4b and d). For composite C (55 vol % AlON) the γ-spinel content is not much affected by deformation, while the δ-oxynitride has almost completely disappeared. Some aluminium nitride is also detected after deformation under 30 MPa. This unexpected decrease of AlON content during creep deformation is more pronounced and easily observable in B material, with probably not much interference with δ-oxynitride phase as in the C composition.

We have therefore focused the TEM observations on B material (33 vol % AlON) to get some more experimental details of this phenomenon. In the as-hot-pressed material B the alumina grains present no defects or dislocations. The Al_2O_3–Al_2O_3 and Al_2O_3-γ-AlON boundaries present no glassy phase.

In the initial material the γ-AlON grains present a lot of defects in the form of little platelets (Fig. 5). The corresponding diffraction patterns show satellite points around those corresponding to some planes (for example (2 2 0)). These defects are not yet analysed, but by analogy with the Al_2O_3–MgO system [13,14] and previous work on the γ-AlON spinel [12], we propose an explanation for these defects.

As previously mentioned in the material description, the γ-AlON phase should be rich in Al_2O_3 and in a metastable state. However, according to Bassoul *et al.* [12] this supersaturated spinel is metastable and thermal treatment can decompose it with the formation of intermediate phases:

(i) ε phases: antiphase periodic structure formed in the (3 1 0) plane of the spinel.

(ii) spinel phases $5AlN \cdot Al_2O_3$, or monoclinic $13Al_2O_3 \cdot AlN$ as described by Michel [15].

During the sintering treatment at 1800 °C, the spinel phase thus dissolves alumina. Our samples are cooled slowly enough to allow a partial decomposition of the γ-spinel phase to the equilibrium phases spinel + alumina; the resulting γ-AlON contains the intermediate phases described before, that would correspond to the defects we observe.

Such explanations are also supported by comparison with work on spinel $MgAl_2O_4$ saturated in alumina [13, 14, 16, 17]. As shown on the MgO–Al_2O_3 diagram [11] the spinel $MgAl_2O_4$ can dissolve a lot of alumina. Lewis [13] and Bansal and Heuer [14] showed that this supersaturated spinel is decomposed (like the oxynitride) by heat treatment, following these precipitation stages:

Stage I: precipitation of spherical particles ($\approx$ 10 nm) that gives a granular aspect on the TEM micrographs.

Stage II: precipitation of particles with a plate-like morphology on some planes, near dislocations.

Stage III: final precipitation of α-Al_2O_3.

According to these TEM observations, we propose that the fine platelets which are observed in the B initial sample would correspond to the second stage of precipitation (no granular aspect is observed in this sample; under other sintering conditions this was seen [1]). Some nitrogen-poor spinel precipitates in the γ-AlON grain, corresponding to the satellite points observed; these precipitates would therefore be coherent with the matrix.

After annealing treatment at 1650 °C and comparing with the initial sample, the precipitates observed in the oxynitride grains (Fig. 6) are more developed, in the form of platelets about 0.1 μm thick and 0.5–1 μm long. These defects could be α-Al_2O_3 precipitates (stage III), because the annealing treatment at 1650 °C (150 °C below the sintering temperature) permits continuing decomposition of the

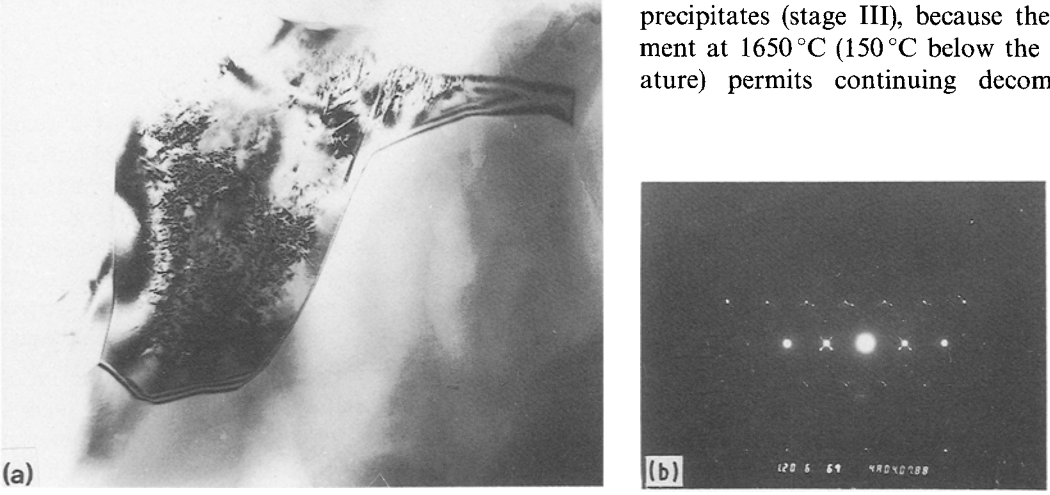

Figure 5 TEM observations of initial (I) B composite: (a) AlON grain and (b) corresponding microdiffraction pattern.

supersaturated metastable spinel formed during the sintering time at 1800 °C.

In Fig. 7, after deformation the B material presents a lot of holes and some microcracks. This underlines the brittleness of this material, which was damaged during the thinning procedure. Some triangular holes at triple points can be due to creep cavities. The spinel oxynitride grains have a different aspect to those observed in the annealed sample (Fig. 6). The composite present only a few grains containing precipitates, as in the initial material. The other γ-AlON grains present no defects. The deformed sample shows a lot of relatively large (3–6 μm) alumina grains, containing small nodules (0.1 to 0.5 μm diameter, Fig. 8). In this B sample, the γ-AlON decomposition is more important (XRD and microstructure) and the alumina platelets which could be formed have coalesced with the previous Al_2O_3 matrix grains. The small intragranular nodules could be nitrogen-poor AlON, or even AlN (its content is too small to be detected by XRD), which is the ultimate stage of γ-oxynitride decomposition (Fig. 8).

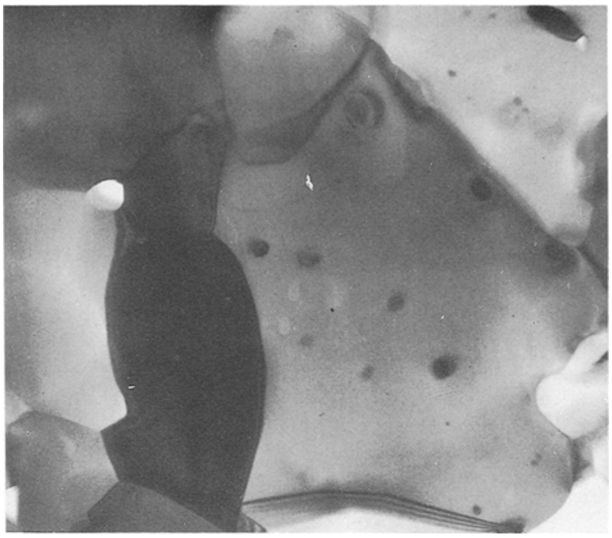

Figure 8 TEM observations of deformed (D) B composite: detail of alumina grains containing nodules.

Figure 6 TEM observation of annealed (T) B composite: AlON grain.

Figure 7 TEM observation of deformed (D) B composite: general view showing cracks and holes.

These TEM observations confirm that the deformation treatment under stress at 1650 °C enhanced the precipitation of the alumina in solution in the γ-AlON spinel. Lewis [13], in the description of his experimental technique, mentioned that due to the structure sensitivity of nucleation of the second-phase particles, it was found convenient to increase the dislocation density in the crystals by deformation prior to ageing at lower temperature. Although nothing is known about dislocation activities in the γ-AlON phase, we can propose that this enhancement of γ-AlON decomposition results in the presence of transgranular dislocations in the AlON grains due to the deformation which promotes or modifies the Al_2O_3 precipitation process. In a study on superplastic deformation in fine-grained $MgO \cdot 2Al_2O_3$ spinel, Panda *et al.* [17] showed that a dynamic recrystallization process occurs during deformation and the dynamic precipitation of Al_2O_3 leads to some decrease in flow stress. By analogy with our study the dynamic precipitation of Al_2O_3 could be at the origin of the slight increase in strain rate during creep.

5. Conclusion

It has been established that during the sintering of the Al_2O_3–γ-AlON composites, the γ-AlON phase was supersaturated in alumina. The metastable phase can be decomposed more by thermomechanical treatment than by thermal treatment. This leads to the precipitation of alumina or AlON spinel with a low nitrogen content. The plasticity of such composite materials could be due more to dislocation activity in the metastable AlON phase than to the classical grain boundary sliding in superplastic ceramic materials.

Acknowledgement

The authors thank Miss A. Fourdeux for helpful discussions on TEM studies.

References

1. D. GOEURIOT, PhD thesis, Lyon, France (1987).
2. D. GOEURIOT, P. GOEURIOT, F. THEVENOT, G. ORANGE, G. FANTOZZI, R. TRABELSI and D. TREHEUX, *Ceram. Internat.* **15** (1989) 207.
3. R. TRABELSI, D. TREHEUX, D. GOEURIOT-LAUNAY, P. GOEURIOT, F. THEVENOT, G. ORANGE and G. FANTOZZI, in Proceedings, 6th CIMTEC, Milan, 1986, edited by P. Vincenzini (Elsevier, Amsterdam, 1986).
4. D. LAUNAY, G. ORANGE, P. GOEURIOT, F. THEVENOT and G. FANTOZZI, *J. Mater. Sci. Lett.* **3** (1984) 890.
5. F. WAKAI, S. SAKAGUCHI and Y. NATSUNO, *Adv. Ceram. Mater.* **1** (1986) 721.
6. T. G. NIEH, C. M. McNALLY and J. WADSWORTH, *Scripta Metall.* **23** (1989) 457.
7. J. D. FRIDEZ, C. CARRY and A. MOCELLIN, in "Advances in Ceramics", Vol. 10 (American Ceramic Society, Mass., USA 1985) p. 720.
8. C. CARRY, in Proceedings of MRS International Meeting on Advanced Materials, Vol. 7, "Superplasticity" edited by M. Kobayashi and F. Wakai (Materials Research Society, Tokyo, Japan, 1989) pp. 199–215.
9. P. C. PANDA, R. RAJ and P. E. D. MORGAN, *J. Amer. Ceram. Soc.* **68** (1985) 522.
10. J. W. Mc CAULEY and N. D. CORBIN, in Proceedings of NATO Advanced Ceramics Meeting, Sussex, UK, July 1981; "Progress in Nitrogen Ceramics", edited by F. L. Riley (Nijhoff, Boston, 1983) pp. 111–118.
11. A. H. HEUER, N. J. TIGHE and R. M. CANNON, *J. Amer. Ceram. Soc.* **63** (1980) 53.
12. D. BASSOUL, A. LEFEVRE and J. C. GILLES, *Mater. Res. Bull.* **11** (1976) 12.
13. M. H. LEWIS, *Phil. Mag.* **20** (1969) 985.
14. E. K. BANSAL and A. H. HEUER, *ibid.* **29** (1974) 709.
15. D. MICHEL, *Rev. Int. Htes Temp. Refract.* **9** (1972) 225.
16. P. C. PANDA and R. RAJ, *J. Amer. Ceram. Soc.* **69** (1986) 365.
17. P. C. PANDA, R. RAJ and P. E. D. MORGAN, *ibid.* **68** (1985) 522.

Received 8 May 1990
and accepted 15 January 1991